ESRF	**Experiment title:** In situ transmission surface diffraction with sub-micrometer spatial resolution: method development and application to studies of transition metal dichalcogenides	**Experiment number**: MI-1299
Beamline: ID31	**Date of experiment**: from: 2018-02-14 to: 2018-02-20	**Date of report**: 2018-05-03
Shifts: 18	**Local contact(s)**: Jakub Drnec	*Received at ESRF:*

Names and affiliations of applicants (* indicates experimentalists):

Tim Wiegmann[1,2*], Finn Reikowski[1*], Fouad Maroun[3*], Jakub Drnec[2*], Olaf Magnussen[1*], Jochim Stettner[1], Philippe Allongue[3]

1: Institut für Experimentelle und Angewandte Physik, Christian-Albrechts-Universität zu Kiel, Leibnizstraße 19, 24118 Kiel, Germany
2: Experimental Division, European Synchrotron Radiation Facility, 71 Avenue des Martyrs, 38043 Grenoble Cedex 9, France
3: Physique de la Matière Condensée, Ecole Polytechnique, 91128 Palaiseau, France

Report:

Introduction: Transmission Surface Diffraction is a novel technique for in situ studies of heterogeneous electrochemical interfaces. It uses high energy photons (40 - 70 keV) and a LEED-like transmission geometry for single-shot projection of the in-plane atomic structure onto a large 2D detector. Proof-of-principle studies conducted during experiments IHCH-1022 and IHCH-1063 have demonstrated surface sensitivity down to partial monolayers for heavy scatterers (Au, Bi). [1] In experiments MI-1251 and MI-1277, we combined TSD measurements with a thin layer flow cell to acquire surface structure information of heterogeneous thin film electrodeposits with micrometre spatial resolution. A publication is in preparation.
In this experiment, TSD was employed for the study of transition metal dichalcogenides (TMDs), which are of high scientific relevance due to their performance as HER catalysts or as battery materials. In particular, we investigated the effects of Cu electrodeposition on 1T-TaS_2, which is known to promote the formation of micrometre-sized nanotunnel networks on the electrode surface. [2] We specifically aimed to show in situ evidence of Cu intercalation into the TMD lattice, which has been proposed as the driving mechanism for the nanotunnel formation.

Experimental details: All experiments were performed in an improved version of the thin layer flow cell developed for our earlier experiments MI-1251 and MI-1277, which features a 4 mm × 2 mm × 0.5 mm channel to achieve laminar flow of electrolyte and is connected to a remote-controlled electrolyte exchange system operating at typical speeds of 1 µl/s. A 0.1 M $HClO_4$ solution was used as supporting electrolyte. For Cu electrodeposition, 10 mM $CuCl_2$ was added. We used a photon energy of 70 keV and beam sizes of either 100 × 500 µm² for general measurements or 5 × 20 µm² for spatially resolved mapping.

Results: 1T-TaS_2 samples were prepared in two different ways, either by peeling thin sheets from single crystals using adhesive tape (resulting in sample thicknesses of a few 10 µm) or by cutting small, 100-500 µm thick pieces off single crystals. Sheets peeled with adhesive tape showeded very heterogeneous surfaces with

many tilted regions, as evidenced by 2D mapping and by the frequent occurance of split peaks at Bragg or CTR positions even when using the focused beam. Charge density wave (CDW) satellite peaks were weak or absent on these samples. The thicker single crystal samples exhibited much smoother surfaces and showed a pronounced CDW signal (Fig. 1).

Cu deposition was performed in stagnant solution at -0.5 V vs. Ag/AgCl. After deposition, a holding potential of 0.05 V was set during the introduction of Cu-free electrolyte. After-deposition measurements were then performed at a potential of -0.2 V.

We observed reproducible structural changes along the 1T-TaS_2 second-order CTRs as a result of Cu deposition, which we attribute to Cu intercalation into the TMD lattice. In particular, additional peaks emerged at L = 0.33, 1.33 along the (2,0), (-2, 2) and other symmetry-equivalent rods and at L = -0.33, 0.66 for the (2, -2) and (-2, 0) family of rods (Fig. 2), growing with increasing Cu coverage. We also observed a slight shift to smaller L-values as a function of total Cu deposition time, with e.g. an intercalation peak appearing at (2,0,0.35) after 5 min of Cu deposition and eventually shifting to (2,0,0.33) after an additional 15 min of deposition time. A similar shift to lower q-values was also observed, less pronounced, for the in-plane peak position. No additional diffraction was observed along first-order CTRs.

Operando monitoring of the 1T-TaS_2 peaks at Bragg positions during square-wave pulse deposition of Cu also showed intercalation-induced structure changes in the bulk crystal, e.g. a 0.06 % decrease in in-plane tensile strain (Fig. 3). The rate of these changes followed a linear decay.

The Cu deposit was stripped by ramping the potential to 0.4 V, with no immediate effect on the aforementioned intercalation peaks. However, we observed these peaks to eventually decay to zero on timescales of 45 - 90 minutes, indicating slow deintercalation.

To demonstrate the possibility of acquiring structure information from isolated single sheets of 1T-TaS_2, an arrangement of five different sheets with varying sizes (50 – 500 µm) and thicknesses (10 - 100 nm) was mounted inside of a 200 µm pinhole and subsequently mapped in air using the focused beam. We found that focusing using only the T2 transfocator (without an additional set of Al CRLs) produced a beam with wide (> 100 µm) tails, meaning that diffraction from the largest, thickest flake(s) would be visible over the whole map. Still, we were able to identify additional peaks with rotation offsets of 0.1° and 60° against the most dominant peak, which exhibited very different spatial dependences and can therefore be attributed to differently oriented sheets (Fig. 4).

Conclusion:

Our experiments showed pronounced and reproducible structural changes in 1T-TaS_2 during Cu deposition, which we attribute to intercalation. A detailed analysis of these effects is in progress. We also demonstrated spatially resolved diffraction from single 1T-TaS_2 flakes. In the future, better focussing (particularly the removal of beam tails) will allow us to access data from even smaller and thinner single sheets.

References

[1] F. Reikowski et al.: *J. Phys. Chem. Lett.* **8**, 1067 (2017)

[2] S. Kumar et al.: *J. Electrochem. Soc.* **155**, 666 (2008)

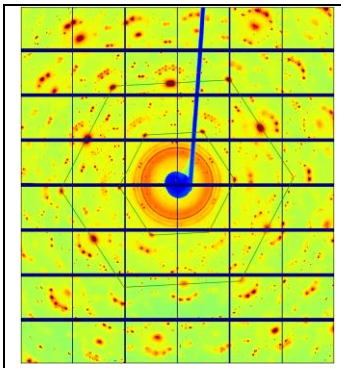

Fig. 1: TSD from 1T-TaS_2 in air, with satellite peaks from CDWs.

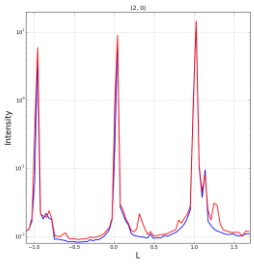

Fig. 2: 1T-TaS_2 (2,0) CTR before (blue) and after (red) 5 min of Cu deposition.

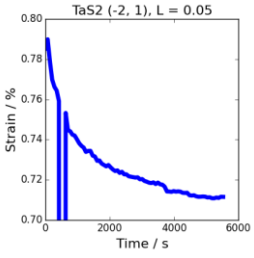

Fig. 3: In-plane tensile strain of the 1T-TaS_2 (-2,1,0) bulk peak during repeated Cu deposition.

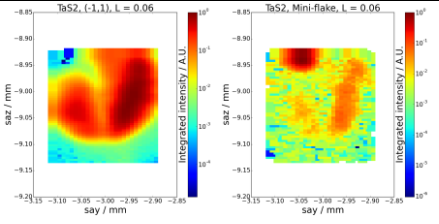

Fig. 4: Real-space map of the integrated intensity for the 1T-TaS_2 (-1,1,0) peak oriented at 0° (left) and 0.1° (right) with respect to the most dominant domain orientation. The two peaks have a different spatial dependence.